RC 22583 (W0210-044) October 4, 2002
Chemistry

IBM Research Report

Enhancement of KRS-XE for 50 keV Advanced Mask Making Applications

Karen Petrillo, David Medeiros, James Bucchignano, Marie Angelopoulos, Dario Goldfarb
IBM Research Division
Thomas J. Watson Research Center
P.O. Box 218
Yorktown Heights, NY 10598

Wu-Song Huang, Wayne Moreau, Robert Lang
IBM Microelectronics Division
Hopewell Junction, NY 12533

Chester Huang, Christina Deverich, Tom Cardinali
IBM Microelectronics Division/MCOC
Essex Junction, VT 05452

Research Division
Almaden - Austin - Beijing - Haifa - India - T. J. Watson - Tokyo - Zurich

Enhancement of KRS-XE for 50 keV Advanced Mask Making Applications

Karen Petrillo, David Medeiros, Jim Bucchignano, Marie Angelopoulos, Dario Goldfarb,*Wu-Song Huang, *Wayne Moreau, *Robert Lang, †Chester Huang, †Christina Deverich, †Tom Cardinali
IBM, T. J. Watson Research Center, Yorktown Heights, NY 10598
*IBM, Microelectronics Division, Hopewell Junction, NY 12533
†IBM Microelectronics Division/MCOC, Essex Junction, VT 05452

ABSTRACT

KRS-XE, a high performance chemically amplified photoresist designed specifically for e-beam mask making applications, has been enhanced to achieve reduced "footing" on chrome oxide surfaces while still maintaining the original lithographic characteristics that make KRS-XE a promising mask making candidate. These attributes include high resolution, superior bake latitudes, high vacuum stability, coated shelf life of greater then 2 months, and, most notably, the absence of a post exposure bake. In conjunction with the footing reduction the requisite sensitivity requirement of <10uC/cm2 with 50 keV exposure tools has been achieved while retaining the robust process latitude previously reported for this resist. Through a careful study of the photoresist formulation components a route to ultra-high sensitivity of <2.5uC/cm2 at 50 keV has been elucidated which will further enhance throughput, decrease heating effects, and potentially be a suitable resist for e-beam projection lithography (EPL.)

Keywords: chemically amplified resist, photomask, e-beam lithography

1. INTRODUCTION

Footing and residual resist material on the chrome oxynitride surface are well known problems with chemically amplified resists (CAR), and have been hypothesized to be related to acid behavior at the chrome/resist interface[1] or the highly polar nature of the chrome oxynitride surface[2]. The problems associated with the footing are numerous, and have in some cases delayed or discouraged mask manufacturers from CAR implementation even though the benefits have been amply illustrated[3 - 5]. Issues include the need for an effective descum procedure that completely removes all footing and residuals. Footing is typically inconsistent from reticle to reticle, dependent on any number of parameters such as the clean room environment, humidity, and cleanliness of the chrome substrate. The footing inconsistency necessitates an aggressive descum, unfortunately this is usually accompanied by an increased etch bias. When targeting small dimensions for assist features and for the 65 nm node, etch biases must be minimized in order to meet resolution requirements and this is contradictory with the descum requirements for resists exhibiting footing problems. Another concern with resist residuals is that they increase the likelihood of defects, an obstacle that mask manufacturers cannot afford. As the footing profile is generally irregular, it introduces a source of line edge roughness (LER) and this roughness is transferred into the chrome during the etch process. Not only does the roughness decrease the CD uniformity on the reticle, which is a major issue in itself, the dimensional irregularities can impact the CD control and LER on the wafer[6].

The wafer industry has been using chemically amplified resists for over a decade, and many of the problems associated with their usage have been thoroughly investigated. Therefore it is not unreasonable to examine the solutions used in the wafer fabs for possible implementation in mask making. Resist footing and scumming from underlying films such as nitride, titanium nitride, and boron phosphorous silicate glass (BPSG) are well known to the wafer industry, and the issue was addressed in two ways. The use of bottom arcs to provide the dual functions of reflectivity control in optical

lithography and act as a barrier layer to prevent interaction or "poisoning" from underlying films are a common solution. Concerns about defects, cost, and process complexity have made the barrier layer concept unattractive for mask making, and only recently have blank suppliers begun to investigate the possibilities[1]. With the introduction of 257 nm laser writing tools the combination bottom arc and barrier layer may gain momentum, but as yet it has not been accepted into manufacturing. A second approach in the wafer industry is to incorporate some type of surface treatment into the process that either quenches basic components on the surface or covers them up with ultra thin films. Deposition of ultra thin oxides[7], oxygen plasma treatments[8], passivation of TiN with hyrdogen[9], cleaning with sulfuric acid mixtures[10], and HCl etching on GaAs substrate[11] have all been proposed. Although these solutions all have merit they add expense and intricacy to the process.

Given the inappropriateness of the wafer fab solutions to the mask making industry, this leaves the photoresist supplier to solve the footing problem through formulation and process improvements. To that end the effect of the photoresist formulation components; photoacid generator (PAG), base, polymer, solvents, and additives have been studied with respect to footing. A suitable solution has been developed to reduce footing on chrome while maintaining the other requisite lithographic attributes that have made KRS-XE a robust mask making resist. Of primary interest to the mask making community are large bake latitudes because of the difficulty of controlling temperature uniformity across a 0.25 inch thick 6 inch glass plate. For chemically amplified resists the most important bake step is the post exposure bake (PEB) because it is in this step that the photo generated acid is diffused through the polymer matrix in the exposed regions, directly impacting linewidth. With KRS-XE the PEB is unnecessary, not only eliminating a process step, but avoiding all of the linewidth control issues associated with the bake. This has proved to be a significant advantage in the NGL reticle arena as well. As Walker[12] discusses, KRS-XE has demonstrated excellent CD uniformity, superior to two competing materials in their evaluation at MCoC, and as a result is being transferred from development to manufacturing. Vacuum stability is another important attribute as mask writing can take as long as 12 to 24 hours per plate. It is important that the resist exposed at the beginning of the write time yield the same critical dimension as the features written towards the end of the exposure. With KRS-XE this has never been an issue because the photochemical reaction requires water to go to completion, hence it can not proceed under vacuum.

Chemically amplified resists offer the combination of sensitivity, contrast, along with high resolution that are essential to answer a critical need for mask makers trying to deal with the complexities of assist features and other OPC strategies. Incorporating knowledge from studies on PAG loading, PAG-to-base ratios, types of bases, base concentrations, and dissolution characteristics[13,14] into the enhanced formulation called KRS-XE3, a resist sensitivity of $<10 uC/cm^2$ on 50 keV exposure tools has been achieved. While this sensitivity is quite acceptable for the current generation of mask writers, ultra high sensitivity is a goal for improved throughput, decreased heating effects, and for future EPL activities. With that in mind, the effects of alternate PAGs, polymer protection levels, and base concentration has been studied to achieve an ultra high sensitivity formulation.

2. EXPERIMENTAL

A proprietary poly(hydroxystyrene)-based polymer in conjunction with the solvent propylene glycol monomethyl ether acetate (PGMEA) as described previously[3] was used in all formulations. Formulations were coated on Hoya AR3 chrome substrates for all of the footing studies, silicon wafers were used for the ultra high sensitivity formulation screening experiments. Resist thickness was measured using a Nanometrics NanoSpec® AFT Model 4000 film thickness measurement tool. Exposures were done on three tools; a 75 keV IBM EL4+ shaped beam mask writer, a 100 keV Leica VB6 direct write tool, and a 25 keV vector scan direct write field emission lithography system (FELS) was used for contrast curves and screening experiments. For the Hoya chrome on glass plates exposed on EL4+, the coatings were done using a CMT/MTC 6000 automated resist coater in conjunction with a Crimson 6000 bake plate with a 0.2 mm proximity gap. Post exposure bakes were not employed, as previously discussed. Development was accomplished using a 0.26 N TMAH solution. Cross-sectional SEM analysis was done on a Hitachi S-4000 scanning electron microscope operating at 10 keV. Resist and chrome linewidth measurements were completed using a KLA 8100 CD SEM. Roughness measurements were performed on a Digital Instruments AFM.

3. RESULTS AND DISCUSSION

3.1 Reduced footing

Although several options for reduced footing were considered including chrome treatments, organic barrier layers, and substrate preparation methods, the upfront approach was a formulation change because this was the easiest for the customer to implement without incurring additional tooling costs, processing steps, or changes in the infrastructure. To tackle the issue it was necessary to quickly determine which formulation component or combination of components was responsible for the footing. There are 4 main components plus small amounts of additives in any chemically amplified photoresist. These include the polymer, photo acid generator (PAG), base, and a solvent system. Of these components, there are innumerable available options in each of the 5 categories eliminating the possibility of screening all options and combinations because of the volumes of experiments that would need to be performed. The strategy that was employed for this work progressed in two phases. The first phase consisted of screening possible component alternatives by looking at contrast curves on AR3 chrome substrates. It was clear from previous evaluations that the contrast curve of KRS-XE on chrome showed an elongated "tail" indicative of a slow-dissolving layer near the substrate, as seen in Figure 1. By making formulation changes which eliminated this "tail" the footing and scumming would be reduced as well. PAGs, bases, and additives were the three formulation components that turned out to be key to reducing the tail on the contrast curve. Broad categories of these three components were evaluated. As seen in the contrast curves, the tail on the contrast curve is greatly reduced or completely eliminated with these formulation changes.

As hypothesized, a clean contrast curve yielded a residue free resist image with reduced footing, but did not necessarily guarantee a vertical profile. Frequently profiles were retrograde, causing image collapse issues at dimensions below 200 nm. Phase 2 of the footing reduction activities involved optimizing the loading of the various components to achieve the required profile. Sensitivity was adjusted to the desired level by implementing solutions learned from the PAG loading, PAG-to-base ratio, quantity and type of base, and dissolution rate studies described previously[11, 12]. Culmination of these efforts afforded residue free vertical profiles with reduced footing as seen in Figure 2. This improved formulation will hereafter be referred to as KRS-XE3.

In order to better characterize the footing on chrome, dissolution studies and AFM roughness analysis were performed on both the base formulation of KRS-XE which has footing issues on chrome, and on the improved formulation, KRS-XE3, with reduced footing and residue. A quartz crystal microbalance[15] (QCM) was used to study the dissolution rate of exposed KRS-XE on two different substrates: one that exhibits footing (CrO) and one that does not (Shipley AR-3 bottom antirflective coating, BARC). Conventional QCM crystals with Au electrodes were customized by either sputtering CrO or spin-casting the BARC directly over the electrode. As can be seen in Figure 3, for the sample on CrO there exists the presence of a regime in the later stages of development, that is near the substrate, at which the rate of dissolution is significantly altered. It appears that as the film dissolves and the thickness decreases to ~60-80 nm, a shift in the development characteristics is observed. No such phenomenon was observed on the sample coated with BARC. Figure 4 shows a SEM images of partially developed KRS-XE on CrO where the presence of this ~70 nm thickness of reduced dissolution rate material can be clearly observed. Evidence of an interfacial layer at the resist/chrome interface was further demonstrated on the KRS-XE samples, exhibiting properties of increased surface roughness and reduced dissolution rate. The interfacial layer consists of residual granules having a thickness of approximately 60 - 70 nm whose density decreases as the exposure dose increases. This interfacial layer corresponds to the tail on the contrast curve as seen in Figure 5a. The KRS-XE3 resist did not exhibit this interfacial layer, and had greatly reduced surface roughness throughout the thickness of the film as seen in Figure 5b. Figure 6 shows an overlay the development rate and the RMS roughness by AFM of a sample of KRS-XE on chrome oxide indicating the concomitant nature of these phenomenon. A surface induced interaction that causes this development shift is proposed although the nature of this interaction has yet to be determined.

3.2 Lithographic Attributes

Qualification of KRS-XE3 was performed using the 75 keV EL4+ mask writer, and one of the first activities was to complete a post apply bake (PAB) optimization to understand the influence of PAB time and temperature on resist

profile. A five point array was designed with 4 corner points and a center position with temperatures ranging from 90 to 110º C, and bake times from 260 to 600 seconds. Results of that study can be found below in Figure 7 where both 100 nm and 300 nm equal line and space features were examined. Although all of the 300 nm features exhibit a vertical profile with reduced footing, the optimum 100 nm feature was found using the 100 º C bake for 430 seconds.

One of the most critical challenges facing the mask making industry with respect to the implementation of chemically amplified resists is to meet or exceed CD uniformity specifications. Vacuum stability is a necessary attribute towards meeting these demands. With extended writing times approaching 12 hours for complex masks, the chemically amplified resist must deliver the same critical dimension across the entire plate regardless of whether it was exposed at time zero or 10 hours later. KRS-XE3 has excellent vacuum stability as evidenced in Figure 8 for write times up 10.8 hours. The average CD had a range of 3 nm over 10.8 hours when the test was terminated.

In addition to vacuum stability, a large dose latitude is an enabler to good CD uniformity. Both isolated and nested features were examined for process window on the 75 keV mask writer at dimensions of 200 and 500 nm. Results in Figure 9 indicate an extensive dose latitude.

3.3 Routes to ultra high sensitivity

In order to achieve ultra high sensitivity a design of experiments (DOE) was performed to understand the formulation space by evaluating characteristics of the 4 main resist constituents: PAG, base, polymer, and solvent system. The experimental matrix contained a fractional factorial array evaluating 4 factors; 2 factors with 3 levels, and 2 factors with 2 levels. SEM micrographs of 100 nm equal line and space features from the 10 samples can be found in Figure 10. The responses for the study were dose latitude, resist profile as related to unexposed dissolution in high normality TMAH developer, sensitivity, and E_0/E_{size}. Table 1 shows the significant factors and their optimum levels. As can be seen there are some conflicts where the optimum levels for one response are not optimum for another response. To establish one optimized formulation the responses were prioritized and some compromises were made. Process window and the unexposed dissolution are the two most important responses. Process window needs to be as large as possible while unexposed dissolution needs to be minimized in order to achieve a square resist profile. The sensitivity goal was less then 10 $\mu C/cm^2$ at 100 keV which is roughly equivalent to less then 5 $\mu C/cm^2$ at 50 keV. Results indicated a sensitivity of less then or equal to 8 $\mu C/cm^2$ at 100 keV was achieved in all cases so tradeoffs could be made with the optimum factors and levels there. E_0/E_{size} is a response that should be less then 1 but it is not the most important factor in the experiment because it can also be adjusted by changing proximity corrections and write bias in the exposure tool. There were no factors that effected E_0/E_{size} at a 95% confidence level in this matrix. To that end, the optimum process from this data is PAG 1 level (+), PAG 2 level (-), base loading level (-), and polymer protection level (+). This combination of factors and levels was actually part of the matrix as experiment 6, and resulted in a 31% dose latitude with 7.4 Å/second unexposed dissolution rate, an E_0/E_{size} of 0.74, and a sensitivity of 3.9 $\mu C/cm^2$. The predicted results from an analysis of the entire matrix indicated that those conditions should result in a 28% dose latitude with a sensitivity of 4.2 $\mu C/cm^2$, an unexposed dissolution rate of 6.2 Å/second and 0.73 E_0/E_{size} ratio. An experiment was done confirming the predicted results with a dose latitude of 29%, and a sensitivity of 4.6 $\mu C/cm^2$ at 100 keV which would translate to approximately 2.3 $\mu C/cm^2$ on a 50 keV mask writer. The unexposed dissolution rate was not measured directly but SEM analysis verified the original square profile as seen in Figure 11.

4. SUMMARY AND CONCLUSIONS

A new version of KRS-XE has been developed which has been enhanced in two respects. Photospeed has been reduced enabling improved throughput on 50 keV mask writers. Additionally, the issue of footing and residue on chrome oxide substrates has been addressed through formulation optimization activities. Demonstration of both attributes is evidenced by the clean square profiles on mask blanks imaged at 4.5 $\mu C/cm^2$ on a 50 keV Leica system and has been accomplished without sacrificing the lithographic performance that KRS-XE is well known for. Most notably these qualities include the absence of a post exposure bake step, large dose latitudes, and excellent vacuum stability. Towards the goal of ultra high sensitivity a formulation has been developed achieving <2.5 $\mu C/cm^2$ sensitivity for 50 keV systems, permitting throughput enhancement, decreased heating effects, and impacting e-beam projection lithography.

ACKNOWLEDGMENTS

The authors would like to thank Kelly Garcia for extensive SEM cross-sectional analysis, and Bill Hinsberg for many useful discussions. We would also like to thank Cecilia Smolinski and Tom Faure of IBM's Burlington Mask House for many valuable discussions, Paul Rabidoux for process support and Mike Trybendis for metrology support. We are pleased to acknowledge the contributions of Eiichi Kobayashi, Nobu Koshiba, and Mark Dennen of JSR. Special thanks to Mathias Irmscher of IMS Chips for the use of his KRS-XE3 images patterned on a 50 keV exposure tool. The authors also gratefully acknowledge DARPA for financial support under Contract Numbers N66001-99-C-8624 and N66001-00-C-8803.

REFERENCES

1. M. Hashimoto, F. Ohta, Y. Yokoya, H. Kobayashi, "CARs blank feasibility study results for the advanced EB reticle fabrication (III)," *Proc. SPIE* , **4409**, pp. 312 - 323, 2001.
2. D. R. Medeiros, "Recent Advances in the Development of Chemically Amplified Resists for Applications in Electron Beam Lithography," *Journal of Photopolymer Science and Technology*, **15**(3), pp 411 - 416, 2002.
3. B. Ashe, C. Deverich, P. Rabidoux, B. Peck, K. Petrillo, M. Angelopoulos, W-S. Huang, W. Moruea, D. Medeiros, "Use of KRS-XE Positive Chemically Amplified Resist for Optical Mask Making," *Proc. SPIE* **4562**, pp. 6640 - 671, 2001.
4. R. Kwong, W.S. Huang, W. Moreau, R. Lang, C. Robinson, D. Medeiros, A. Aviram, R. Guarnieri, M. Angelopoulos, "A new high performance CA resist for E-beam lithography," *Mat. Res. Soc. Symp. Proc*., **584**, p 147, 2000.
5. T. Segawa, M. Kurihara, S. Sasaki, H. Inomata, N. Hayashi, H. Sano, "Performance of positive tone chemically amplified resists for next generation photomask fabrication," *Proc. SPIE*, **3236**, pp. 82 - 93, 1997.
6. P. Yan, G. Zhang "Experimental study of mask line edge roughness transfer in DUV and EUV lithography patterning processes," *Proc. SPIE*, **3873**, pp. 865 - 874, 1999.
7. C. P. Soo, S. Valiyaveettil, A. Huan, A. Wee, T. C. Ang, H. Fan, A. J. Bourdillon, L. H. Chan, "Enhancement or Reduction of Catalytic Dissolution Reaction in Chemically Amplified Resists by Substrate Contaminants," *IEEE Trans. On Semiconductor Manufacturing*, **12**(4), pp. 462 - 469, 1999.
8. S. Mori, T. Watanabe, K. Acachi, T. Fukushima, K. Uda, Y. Sato, "Substrate effect in chemically amplified resist," *Proc SPIE*, **2724**, pp. 131 - 138, 1996.
9. C. H. Lin, C. C. Chen, J. S. Jenq, M. O. De Beek, M. O. Van Den, "DUV resist profile improvement on TiN deposited metal layer," *Proc SPIE*, **2726**, pp. 427 - 436, 1996.
10. S. Mori, T. Fukushima, Y. Sato, "Analysis of substrate effect in chemically amplified resist on silicate glass," *Jpn. J. Appl. Phys*. **35**(12B), pp. 6495 - 6500, 1996.
11. B. Lu, O. Vladimirsky, J. W. Taylor, N. Dandekar, "The importance of surface chemistry of GaAs during chemically amplified resist processing by X ray lithography," *Proc. 1998 GaAs MANTECH Conf*., pp. 221 - 222, 1998.
12. D. Walker, DP Mathur, C. Su, T. Huang, "Application of vector scan electron beam lithography to 45 nm node extreme ultraviolet lithography reticles," Photomask Japan 2002.
13. D. R. Medeiros, K. Petrillo, J. Bucchignano, M. Angelopoulos, W.S. Huang, W. Li, W. Moreau, R. Lang, R. Kwong, C. Magg, B. Ashe, "Extending the performance of KRS-Xe for high throughput electron beam lithography for advanced mask making," *Proc. SPIE*, 4562, pp. 552 - 560, 2001.
14. D. R. Medeiros, K. Petrillo, G. Breyta, W. S. Huang, W. Moreau, "Sensitivity Factors of CAR Electron Beam Resists," *Proc. SPIE*, **4690**, pp. 442 - 453, 2002
15. W. D. Hinsberg, K. K. Kanazawa, "Quartz Crystal Microbalance Thin Film Dissolution Rate Monitor," *Rev. Sci. Instrum.* **60**, 489 - 492, 1989.

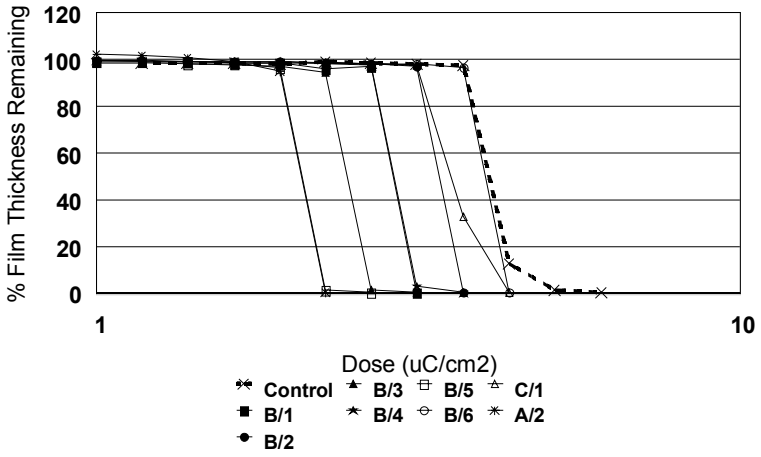

Figure 1. Contrast curves on AR3 chrome from the various formulations: Control is KRS-XE, Component A1 was used in conjunction with all of evaluations of component B.

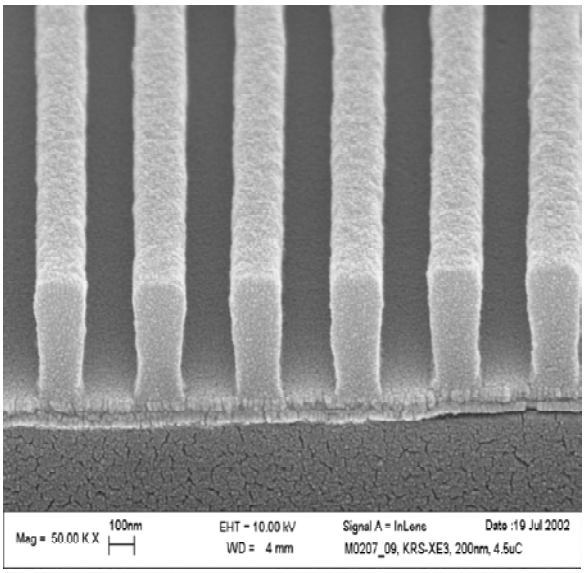

Figure 2. SEM cross sections of KRS-XE3 reduced footing formulation on chrome reticles exposed on a 50 keV Leica tool. 200 nm equal lines and spaces are shown in a 400 nm thick film imaged using a dose of 4.5 $\mu C/cm^2$. Photo courtesy of Mathias Irmscher of IMS Chips.

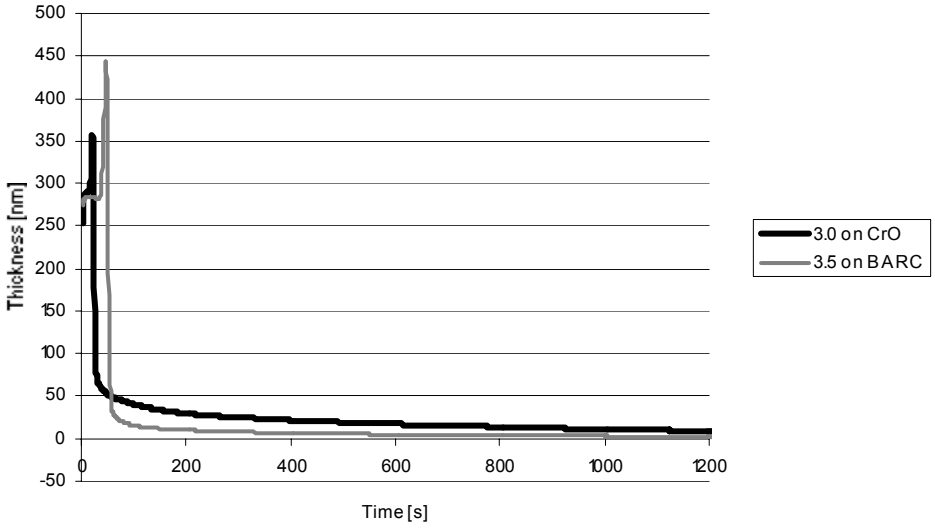

Figure 3. Dissolution rates (QCM) of exposed KRS-XE on CrO and BARC.

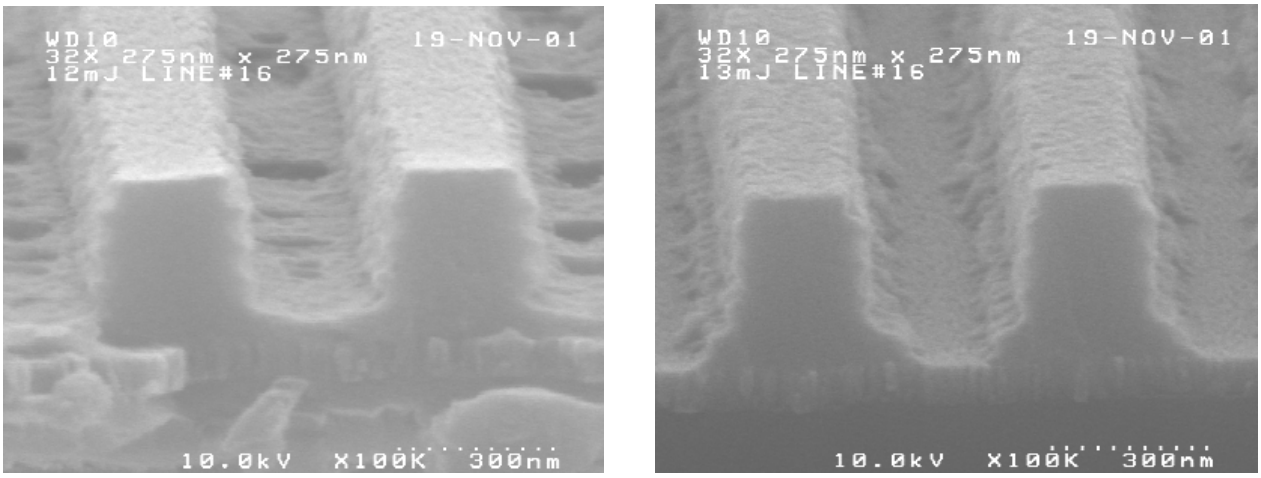

Figure 4. SEM images of partially developed KRS-XE showing presence of slow-developing layer near resist-surface interface.

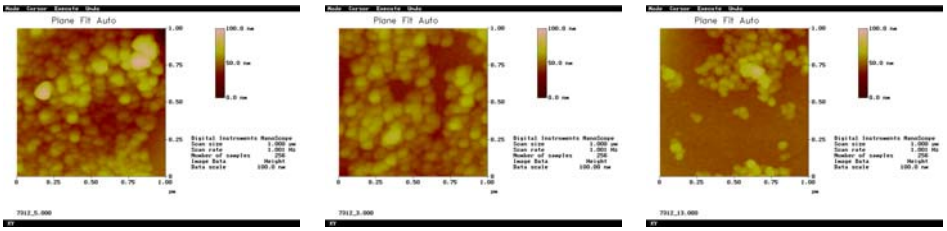

R = 10.7 nm R = 7.3 nm R = 6.7 nm

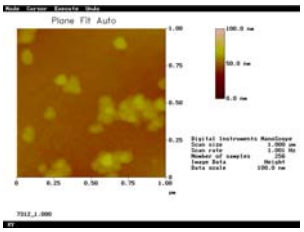

R = 4.0 nm

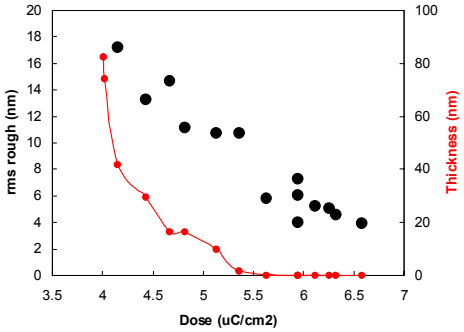

5a. KRS-XE

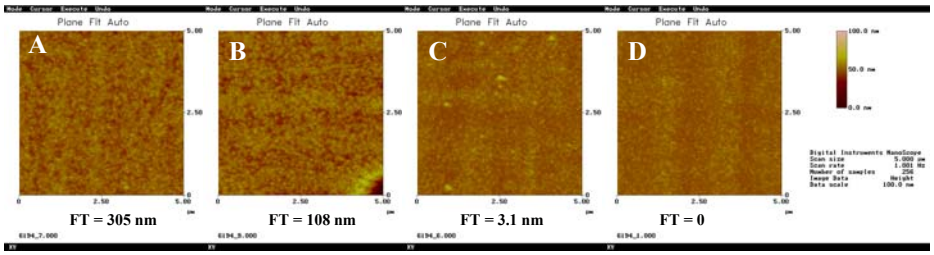

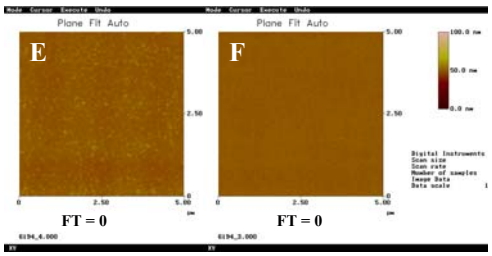

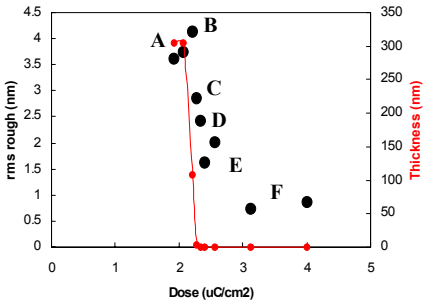

5b. KRS-XE3

Figure 5. AFM roughness measurements of KRS-XE (top) reveal the formation of an interfacial layer, and the absence of that layer with the improved formulation, KRS-XE3 (bottom).

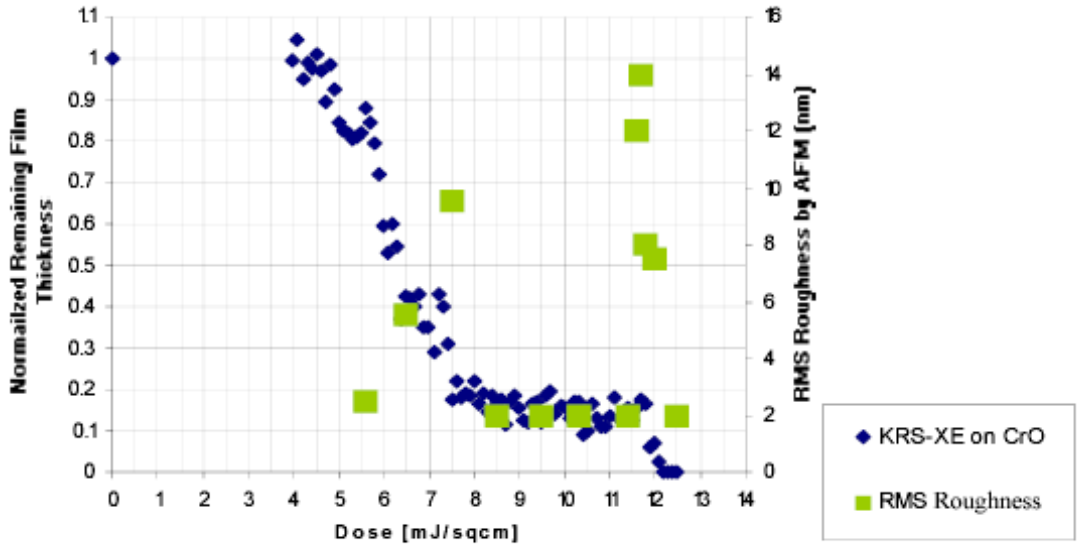

Figure 6. Overlay of dissolution rate (QCM) and RMS roughness (AFM) for exposed KRS-XE.

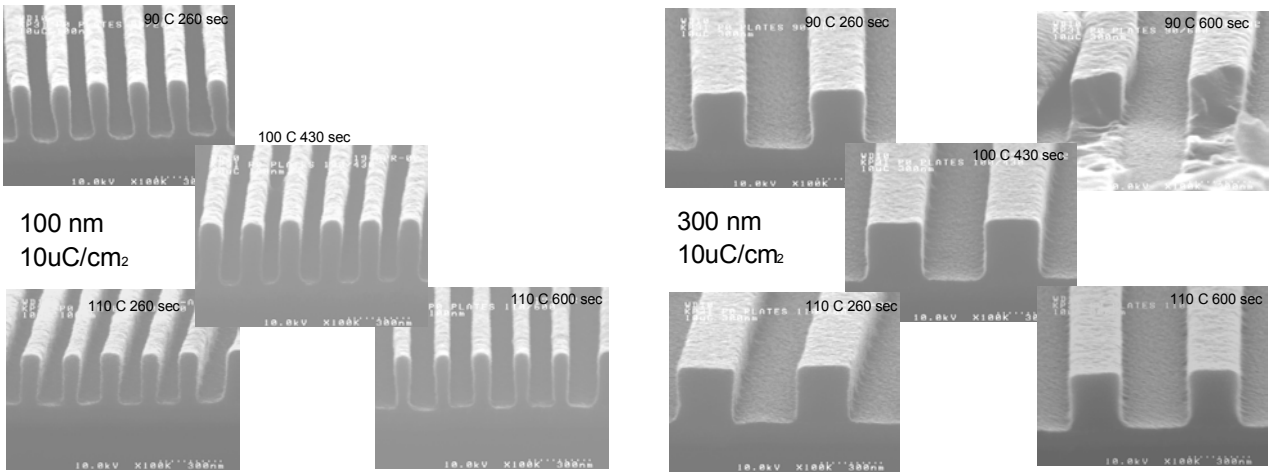

Figure 7. PAB optimization for resist profiles of KRS-XE3 indicate that the optimum bake condition is 100 ° C bake for seconds.

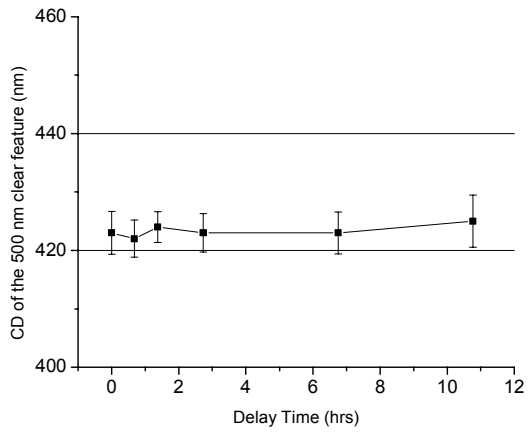

Figure 8. KRS-XE3 has excellent vacuum stability over a 10.8 hr write time.

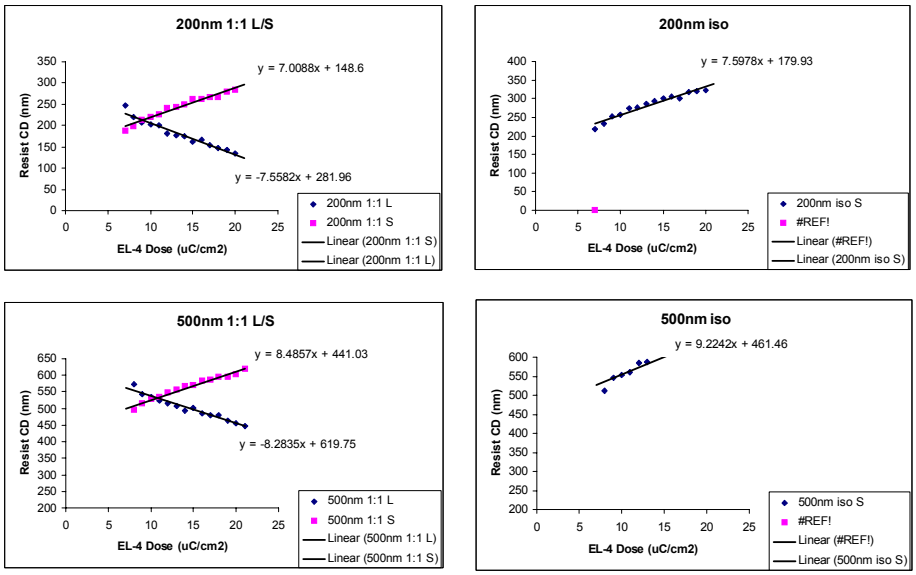

Figure 9. The dose latitude of KRS-XE3 for 200 and 500 nm isolated and dense features enables excellent CD uniformity.

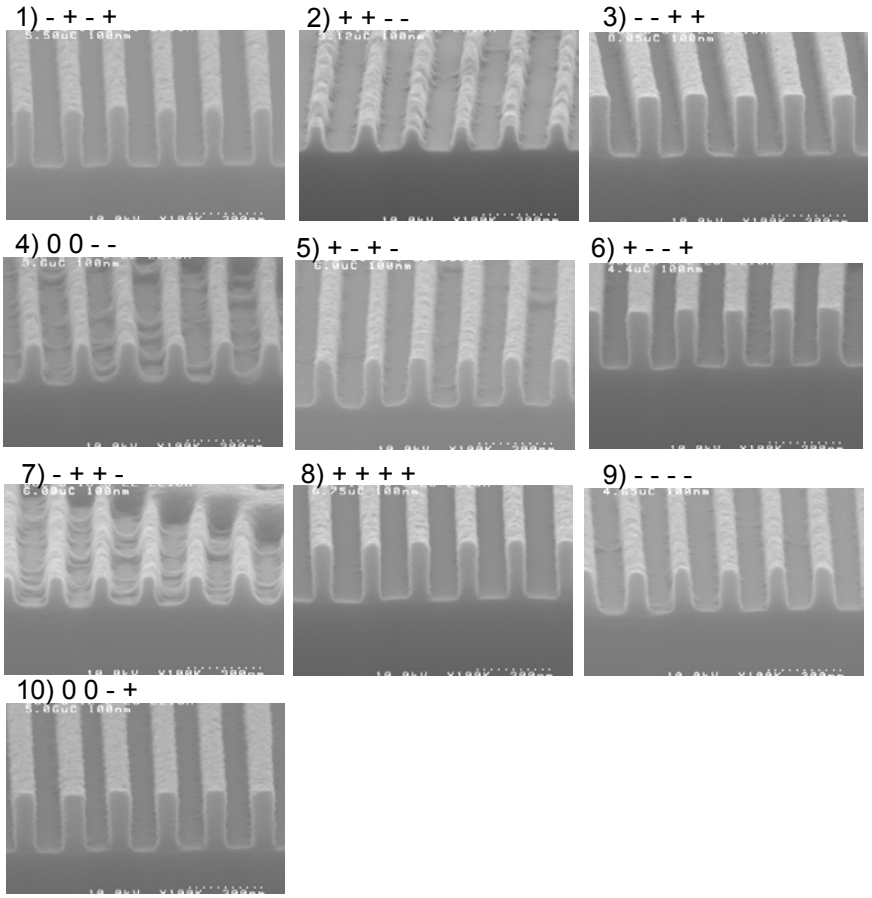

Figure 10. SEM micrographs show resist profiles of the 100 nm equal line and space features from the 10 samples in the matrix. The experiment contained 4 factors, the levels of those factors are indicated by +, 0, and - symbols.

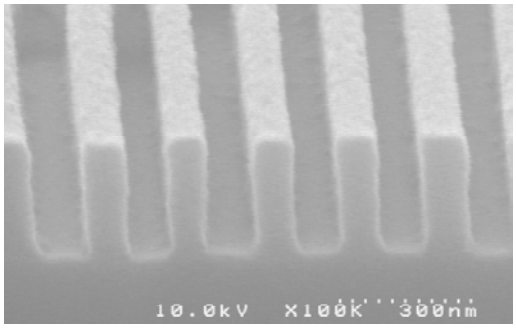

Figure 11. Results of the confirmation experiment exhibit a sensitivity of 4.6 $\mu C/cm^2$ at 100 keV with a large dose latitude.

Factors	**Process Window**	**Unexposed dissolution**	**E_0/E_{size}**	**Sensitivity**
A. PAG 1				3) + Optimum
B. PAG 2	2) - Optimum	2) - Optimum		
C. Base Loading				1) - Optimum
D. Polymer Protection Level	1) + Optimum	1) + Optimum		2) - Optimum
Interaction: 2 PAGS				
Interaction: PAG x Base	3) A -, C + or A +, C - Optimum	3) A -, C + Optimum		

Table 1. The significant factors and their optimum levels to achieve ultra high sensitivity with a large process window.